EurJIC
European Journal of Inorganic Chemistry

Full Papers
doi.org/10.1002/ejic.202100024

Chemistry Europe
European Chemical Societies Publishing

VIP *Very Important Paper*

Synthesis, Characterization, and Evaluation of Antibacterial Activity of Ferrocenyl-1,2,3-Triazoles, Triazolium Salts, and Triazolylidene Complexes of Gold(I) and Silver(I)

Carolin Hoyer,[a] Peter Schwerk,[b] Lisa Suntrup,[a] Julia Beerhues,[c] Maite Nössler,[a] Uta Albold,[a] Jens Dernedde,[d] Karsten Tedin,[b] and Biprajit Sarkar*[a, c]

1,2,3-triazoles, the corresponding triazolium salts, and the resulting mesoionic carbenes (MICs) of the 1,2,3-triazol-5-ylidene type are at the forefront of contemporary research. In this contribution, we present a comprehensive study involving eight triazoles, seventeen triazolium salts, two silver(I)- and four gold(I)-MIC complexes. The substituents on the N1-atom of the heterocycles are either ferrocenyl or phenyl and those on the C4-atom bear various alkyl groups. All the compounds were thoroughly characterized by a combination of multinuclear NMR spectroscopy, ESI-MS and in many cases through single crystal X-ray diffraction studies. In the electrochemical analysis, all ferrocenyl-containing compounds display a ferrocenyl-based oxidation step. Additionally, in both the triazolium salts, and the respective metal complexes, a ligand centered reduction step is observed. All the complexes were tested for their antibacterial properties against the Gram-negative bacterial strains *Salmonella typhimurium* (*S. typhimurium*) and *Escherichia coli* (*E. coli*). Many of the tested compounds display good antibacterial activity against the rather resistant *Salmonella* strain. To inhibit the growth of *E. coli*, higher concentrations of the compounds tested were required. A preliminary structure-activity relationship of this set of compounds is also reported.

Introduction

The copper-catalyzed azide alkyne cycloaddition (CuAAC) reaction,[1] one of the most popular examples of the so-called click reaction,[2] has impacted diverse branches of chemistry in the recent past. In organometallic chemistry, the corresponding 1,2,3-triazol-5-ylidenes, which are derived from the 1,2,3-triazoles synthesized by this click reaction, have established themselves as a popular class of mesoionic carbenes (MICs).[3] Metal complexes of such MICs have not only found use in homogeneous catalysis,[3d,4] but also in various other fields such as electro-active compounds,[5] photochemistry[6] and redox-induced or redox-switchable catalysis.[4e,i,s,7] Gold(I)-MIC complexes display good to excellent catalytic activity in several reactions containing alkynes as substrates.[4s,7b,8] Silver(I) complexes of 1,2,3-triazol-5-ylidenes have been popular because of their relevance in the transmetallation route for synthesizing metal complexes with MICs.[9] Additionally, silver(I)-MIC complexes have also found use in catalysis in their own right.[10]

1,2,3-triazoles have relevance in medicinal chemistry.[11] Furthermore, metal complexes of N-heterocyclic carbenes (NHCs) have recently been extensively tested for their biological activity.[12] In view of the above facts, we were interested in probing the antibacterial effect of 1,2,3-triazoles, the 1,2,3-triazolium salts, as well as the corresponding silver(I)- and gold(I)-MIC complexes. It should be mentioned here that a few 1,2,3-triazolium salts[13] and metal complexes with MIC ligands of the 1,2,3-triazol-5-ylidene type[7b,14] have been tested in the recent past for their biological activity. In the following, we present a comprehensive study that involves eight 1,2,3-triazoles, seventeen 1,2,3-triazolium salts, two silver(I)- and four gold(I) MIC complexes. All the compounds were thoroughly characterized by a combination of multinuclear NMR spectroscopy, ESI-MS, and in several cases through single crystal X-ray diffraction studies. The electrochemical properties of the ferrocenyl derivatives are reported. The antibacterial activity of the compounds against the Gram-negative bacterial strains *S. typhimurium* and *E. coli* are presented. A first and preliminary attempt is made at drawing a structure-activity correlation in terms of antibacterial properties of these compounds.

[a] *C. Hoyer, Dr. L. Suntrup, M. Nössler, Dr. U. Albold, Prof. Dr. B. Sarkar*
Institut für Chemie und Biochemie, Freie Universität Berlin,
Fabeckstrasse 34–36, 14195 Berlin, Germany
[b] *P. Schwerk, Dr. K. Tedin*
Institut für Mikrobiologie und Tierseuchen, Freie Universität Berlin,
Robert-von-Ostertag-Str. 7–13, 14163 Berlin, Germany
[c] *J. Beerhues, Prof. Dr. B. Sarkar*
Lehrstuhl für Anorganische Koordinationschemie, Institut für Anorganische Chemie, Universität Stuttgart,
Pfaffenwaldring 55, 70569 Stuttgart, Germany
E-mail: biprajit.sarkar@iac.uni-stuttgart.de
https://www.iac.uni-stuttgart.de/en/research/aksarkar/
[d] *Dr. J. Dernedde*
Institut für Laboratoriumsmedizin, Klinische Chemie und Pathobiochemie, Charité-Universitätsmedizin Berlin,
Corporate member of Freie Universität Berlin, Humboldt-Universität zu Berlin, and Berlin Institute of Health,
Augustenburger Platz 1, 13353 Berlin, Germany

Supporting information for this article is available on the WWW under https://doi.org/10.1002/ejic.202100024

Synthesis and Characterization

The triazoles were synthesized *via* the CuAAC reaction from the corresponding azides and alkynes in good yield (67–89%). The compounds **1a**[15] and **5a–5c**[16] were previously reported and were re-synthesized for the current work (Scheme 1). The ferrocenyl group was chosen as a substituent on the N1-atom of some of the triazoles (**1a–1e**). This was done as the ferrocenyl group is often considered a privileged motif for creating compounds with biological activity,[17] and also for its additional redox-activity.

For the triazoles **5a–5c**[16] the substituent at the N1-atom is a phenyl group. This was done to have an aromatic, non-ferrocenyl substituent in order to get a sound comparison with the ferrocenyl substituted triazoles. Alkyl substituents were chosen on the C4-atom of all the triazoles, as such substituents showed positive effects[12c,13a,f] on the biological activity of related heterocycles. Additionally, it was planned to introduce an alcohol or a carboxylic acid group on the alkyl substituents (**1c–1e**) in order to increase the water solubility of the respective compounds, and to investigate the influence of a proton source on their bioactivity. As the complex syntheses with these ligand precursors failed and since the ferrocenyl triazoles **1d** and **1e** themselves did not show significant antibacterial activity against the tested bacterial strains (*vide infra*), only phenyl analogues **5a–5c**[16] were synthesized.

All the triazoles were methylated to the triazolium salts in good yield (58–99%). For the methylation reactions, different methylating reagents such as MeI, MeOTf and Meerwein salt (Me_3OBF_4) were used (Scheme 1). Such an approach allowed us to generate triazolium salts with different counter anions in order to be able to test the effect of these on the biological activity of the triazolium salts. The triazoles and the triazolium salts were characterized by a combination of ^1H and $^{13}C\{^1H\}$ NMR spectroscopy and mass spectrometry. In the ^1H NMR spectra of the triazoles, the resonance of the C–H triazole ring proton appears downfield shifted between 7.50 and 8.22 ppm, and is very characteristic for this class of compounds.[18] On

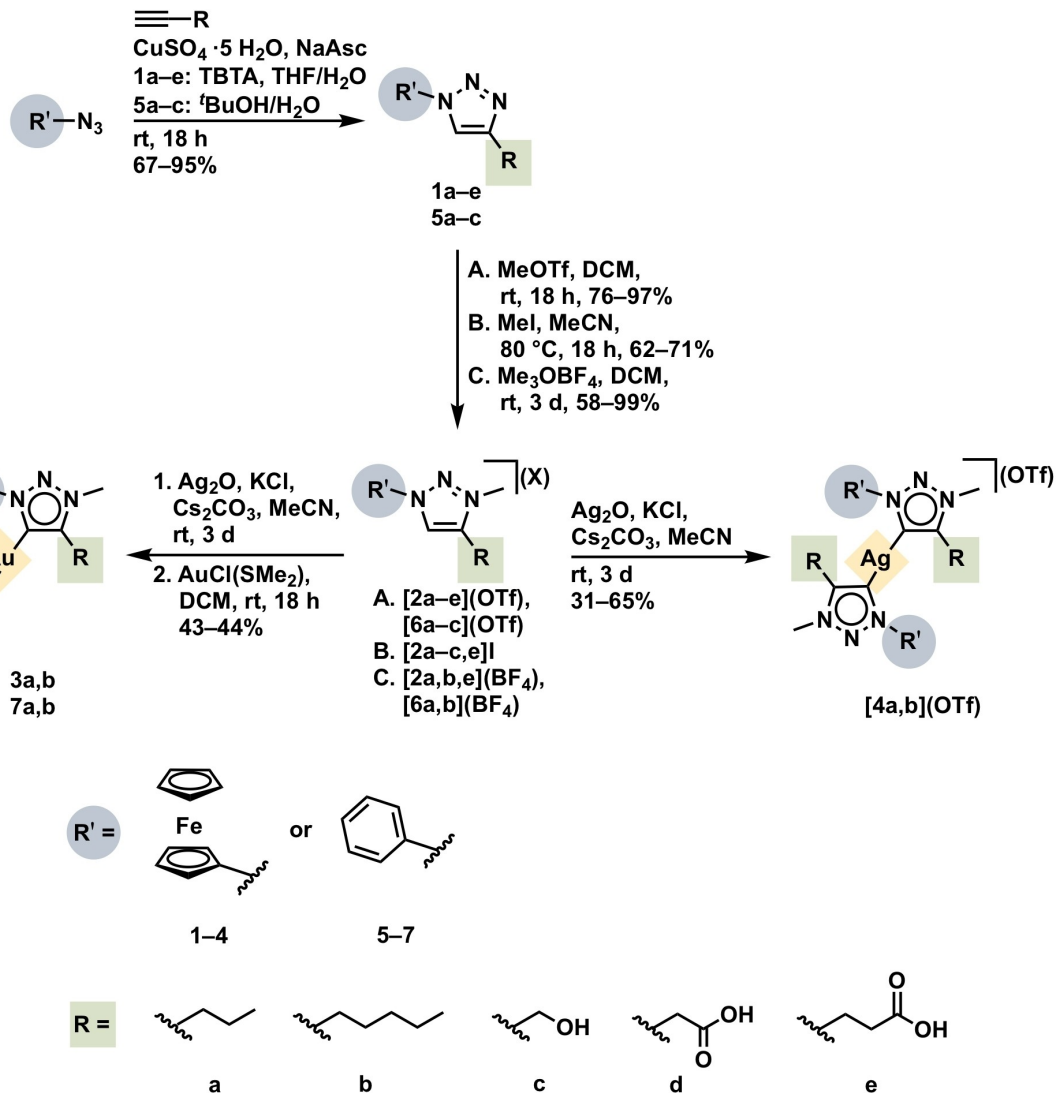

Scheme 1. Synthetic route starting from the respective azides and alkynes. Compounds **1a**[15] and **5a–c**[16] are literature known.

Full Papers
doi.org/10.1002/ejic.202100024

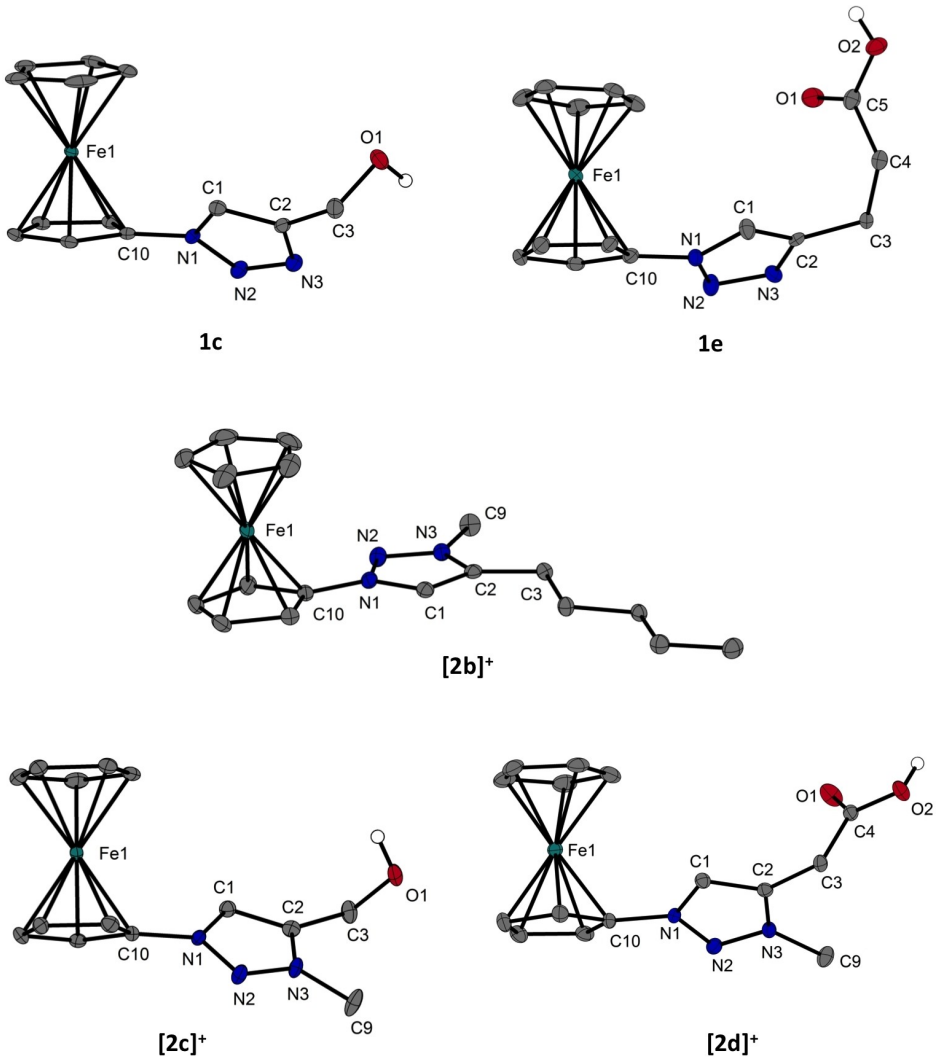

Figure 1. Molecular structures in the crystal of triazoles **1 c** and **1 e** and triazolium salts **[2 b](OTf)**, **[2 c](OTf)** and **[2 d](OTf)**. Ellipsoids are rendered at 50% probability level. Hydrogen atoms (except for the OH groups) and counter ions have been omitted for clarity.

methylation, the signal for the triazolium ring C–H proton is further downfield shifted and appears between 9.00 and 9.60 ppm. The shift of this aforementioned signal is usually a good indication for the formation of the triazolium salts.[19] In the ESI-MS the triazoles usually delivered a peak in the protonated form or with Na^+. For the triazolium salts the molecular peak corresponding to the triazolium cation was clearly observed in the ESI-MS.

Single crystals suitable for X-ray diffraction studies could be obtained for the triazoles **1 c** and **1 e**, and for the triazolium salts **[2 b](OTf)**, **[2 c](OTf)** and **[2 d](OTf)** (Figure 1). As was reported previously, in the molecular structures of the triazoles in the crystal, the central N2–N3 bond is shorter compared to the two bonds that flank it (Table 1),[7a,20] pointing to a localized bond situation inside the triazole ring. On methylation to the triazolium salts, the bond lengths within the triazolium ring become more equal, indicating a more delocalized situation (Table 1).

Table 1. Selected bond lengths (Å) of **1 c**, **1 e**, **[2 b](OTf)**, **[2 c](OTf)** and **[2 d](OTf)**.

	Bond length [Å]				
Bond	**1 c**	**1 e**	**[2 b](OTf)**	**[2 c](OTf)**	**[2 d](OTf)**
N1–N2	1.351(2)	1.337(6)	1.325(3)	1.329(2)	1.321(3)
N2–N3	1.316(2)	1.328(6)	1.326(3)	1.329(2)	1.323(3)
N1–C1	1.354(2)	1.355(6)	1.355(3)	1.354(3)	1.364(3)

The triazole and triazolium rings are twisted with respect to the connected Cp-ring with a dihedral angle ranging from 3 to 46°. The two Cp rings in the compounds take up conformations from almost perfectly eclipsed (**1 e** and **[2 c](OTf)**) to a more staggered situation (**1 c**, **[2 b](OTf)** and **[2 c](OTf)**).

The gold(I) complexes **3 a**, **b** and **7 a**, **b** were synthesized *via* the Ag(I)-mediated transmetallation route in reasonable yield (Scheme 1). The disappearance of the signal corresponding to the ring C–H proton of the triazolium ring is a good indication for the formation of such MIC complexes. The carbene-C signals

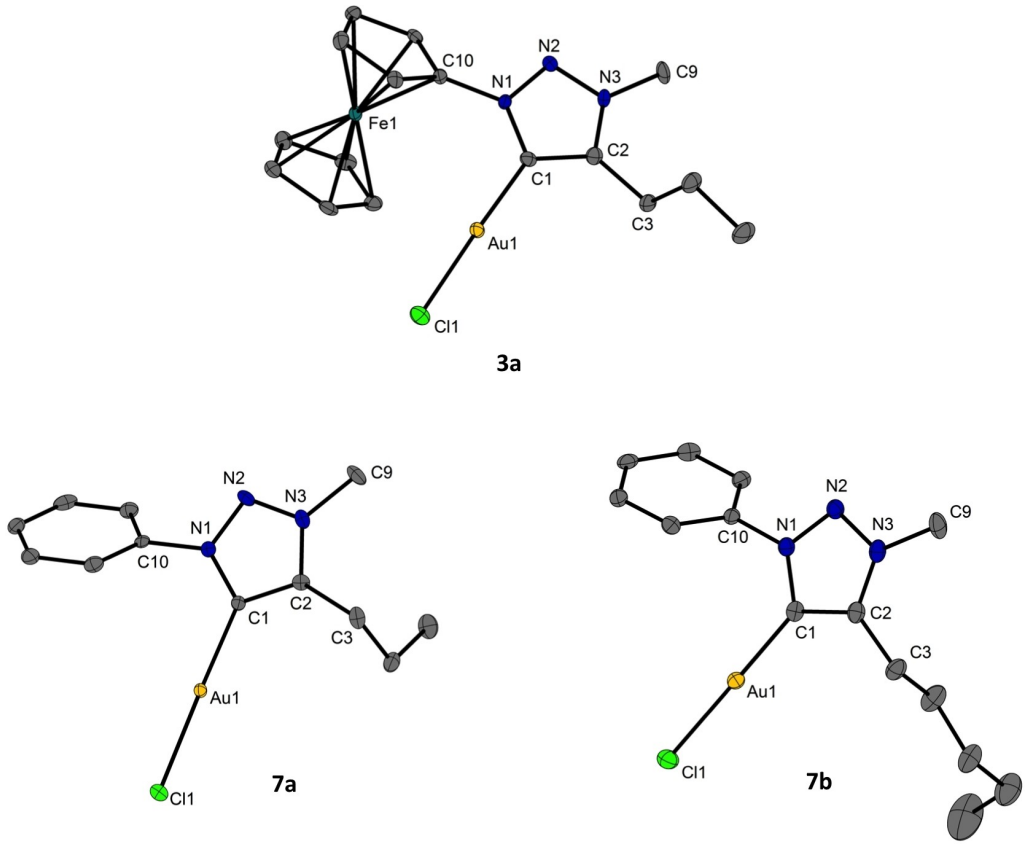

Figure 2. Molecular structures in the crystal of gold(I)-MIC complexes **3a**, **7a** and **7b**. Ellipsoids are rendered at 50% probability level. Hydrogen atoms have been omitted for clarity.

in the $^{13}C\{^1H\}$ NMR spectra of the compounds were observed between 156.0 and 157.6 ppm. In the ESI-MS of **3a** and **3b** a peak corresponding to the cation after loss of the Cl^- was observed. For the complexes **7a** and **7b** the peak for the respective cationic complex with two triazolylidene ligands was detected. Unfortunately, the isolation of the gold complexes *via* the transmetallation route with ligands that contain additional –OH or –COOH functionalities was not successful. Single crystals suitable for X-ray diffraction studies were grown for **3a**, **7a** and **7b** (Figure 2). In the molecular structure in the crystal, the Au(I) center displays a near linear coordination, being coordinated by the carbene-C of the MIC, and by an additional chlorido ligand. The deviation from linearity in the three compounds is between 2–3°. The bond lengths within the triazolylidene ring, as well as the Au–$C_{Carbene}$ and Au–Cl bond lengths are all in the expected range (Table 2).[7a,8b,e,14a,21] The triazolylidene ring of **3a** is twisted with respect to the connected Cp-ring with a dihedral angle of 38°. The angle between the phenyl substituent and the triazolylidene ring in **7a** and **7b** varies from 46 to 56°.

The silver complexes **[4a, b](OTf)** were synthesized by the reaction of Ag_2O and the respective triazolium salt **[2a, b](OTf)** in the presence of KCl and a base (Scheme 1). Despite the presence of excess KCl, we were only able to isolate the homoleptic complexes. The purity and the identity of the silver complexes were established in a similar way as reported for the gold complexes above. Interestingly, for both complexes coupling of the carbene-C to the two naturally occurring silver isotopes, ^{107} Ag and ^{109} Ag, is observed as a doublet due to $J_{(C\text{-}107/109\ Ag)}$ coupling at 165 ppm in the respective $^{13}C\{^1H\}$ NMR spectrum.[12b,22] Just like for the gold complexes, it was not possible to isolate the silver complexes with ligands that contain additional functionalities like –OH and –COOH. For reasons that are not very clear to us, it was also not possible to isolate the silver complexes with triazolylidene ligands that contain a phenyl substituent at the N1-atom (Scheme 1). We were able to obtain single crystals of **[4a](OTf)** and **[4b](OTf)** that were suitable for single crystal X-ray diffraction analysis (Figure 3). In both the compounds, the Ag(I)-center displays a near linear coordination, being coordinated by a carbene-C from each of the MIC ligands. The Ag–$C_{carbene}$ bond lengths in

Table 2. Selected bond lengths (Å) of **3a**, **7a** and **7b**.

Bond	Bond length [Å] **3a**	**7a**	**7b**
N1–N2	1.336(4)	1.330(4)	1.331(5)
N2–N3	1.323(4)	1.311(4)	1.328(5)
N1–C1	1.368(4)	1.373(4)	1.373(6)
Au–C1	1.986(3)	1.986(4)	1.971(5)
Au–Cl	2.291(1)	2.297(9)	2.291(1)

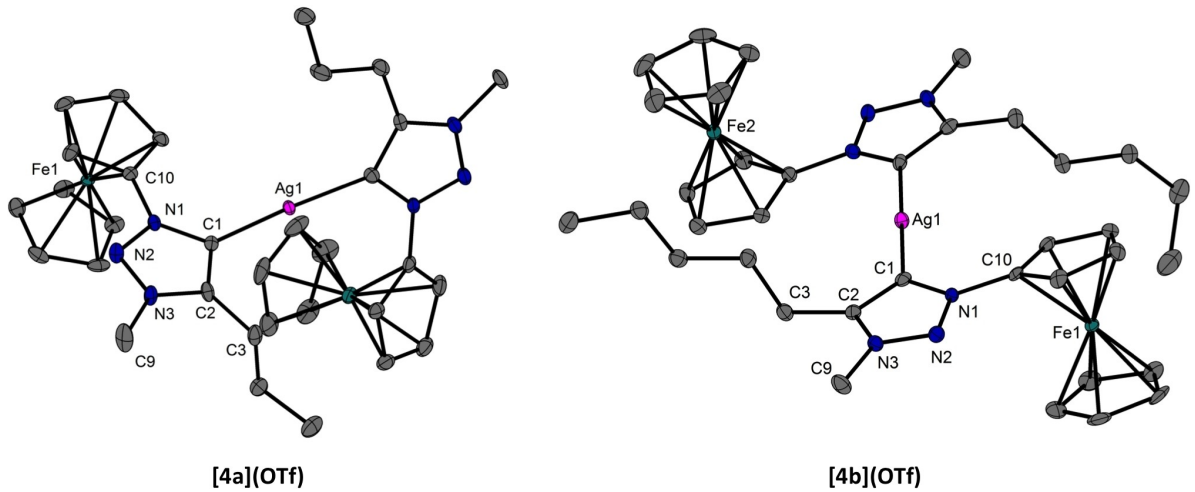

Figure 3. Molecular structures in the crystal of silver(I)-MIC complexes **[4a](OTf)** and **[4b](OTf)**. Ellipsoids are rendered at 50% probability level. Hydrogen atoms and counter ions have been omitted for clarity.

both compounds are in the expected range (Table 3).[4h,23] The conformation of the Cp-rings in the ferrocenyl groups is nearly eclipsed. In both the compounds, the ferrocenyl groups from the two ligands are oriented anti to each other, likely because of steric reasons (Figure 3).

Table 3. Selected bond lengths (Å) of **[4a](OTf)** and **[4b](OTf)**.

Bond	Bond length [Å] **[4a](OTf)**	**[4b](OTf)**
N1–N2	1.340(3)	1.338(3)
N2–N3	1.323(3)	1.320(3)
N1–C1	1.372(3)	1.369(4)
Ag–C1	2.076(2)	2.094(3)

Electrochemistry and Antibacterial Studies

All the ferrocenyl-containing compounds reported here were subjected to cyclic voltammetry measurements in THF/0.1 M Bu_4NPF_6. The compounds all display an oxidation step which is ferrocenyl centered (Figure 4 and Figure S64–66). The substituent on the heterocyclic ring has only a very marginal influence on the oxidation potentials (Table 4). For all the investigated compounds the current heights for the forward and reverse waves of the oxidation step are close to unity, indicating a high degree of reversibility (Table 4). Interestingly, even though the ratio of the current heights is close to unity for the oxidation step, the difference in the potentials of the forward and the

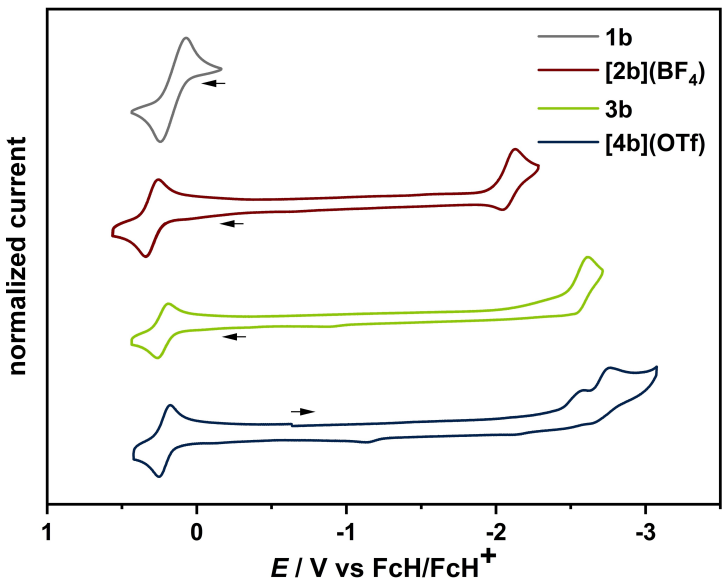

Figure 4. Comparison of the normalized cyclic voltammograms of triazole **1b**, triazolium salt **[2b](BF$_4$)**, Au(I)-MIC complex **3b** and Ag(I)-MIC complex **[4b](OTf)**. All CVs were measured in abs. THF/0.1 M Bu_4NPF_6 with a glassy carbon electrode at a scan rate of 100 mV/s and 295 K.

Table 4. Oxidation potential ($E_{1/2}$), peak-to-peak separation (ΔE) and peak current ratio I_p^{Red}/I_p^{Ox} of the oxidation of all compound classes.

Compound	Oxidation $E_{1/2}$	ΔE	I_p^{Red}/I_p^{Ox}
1a	0.17	0.31	1.06
1b	0.16	0.17	1.06
1c	0.18	0.10	1.01
1d	0.18	0.15	0.97
1e	0.17	0.32	0.99
[2a](BF$_4$)	0.29	0.14	1.07
[2b](BF$_4$)	0.30	0.09	0.94
[2c](OTf)	0.32	0.15	1.03
[2d](OTf)	0.32	0.10	0.97
[2e](BF$_4$)	0.30	0.09	1.01
3a	0.21	0.13	0.93
3b	0.23	0.07	0.94
[4a](OTf)	0.21	0.08	0.94
[4b](OTf)	0.21	0.09	0.91

reverse peak vary quite a bit (Table 4). Ferrocenyl compounds with large substituents often display a large reorganization energy owing to different conformations in the non-oxidized and oxidized forms. Such a conformational change is likely the reason for a somewhat large difference in the forward and the reverse potentials observed for many of the compounds here. The oxidation potentials of the ferrocenyl units shift to the positive direction on moving from the triazoles to the triazolium salts. Such a shift can be attributed to the additional positive charge on the triazolium rings (Table 4). Deprotonation of the triazolium rings and complexation leads to a slight negative shift of the oxidation potentials in comparison to the triazolium salts.

The triazoles do not display any reduction steps within the solvent window of THF. The triazolium salts as well as the metal complexes display one or more irreversible reduction steps (Figure 4). In comparison to related compounds reported earlier, one irreversible reduction can be attributed to the reduction of the triazolium unit, or to the reduction of the triazolylidene ligands.[4e,i,7a] As expected, the reduction of the triazolium salts that contain a direct positive charge on the ring, is shifted towards the positive direction in comparison to the metal complexes in which the triazolylidene rings are formally neutral (Table S10).

All the compounds were tested in an initial screening for their antibacterial activity against the Gram-negative bacterial strain *S. typhimurium* by using a modified liquid microdilution assay (CLSI, 2017;[24] Supporting Information 6.1.1). After this initial screening, all non-effective compounds were excluded from further testing (Figure 5).

As the compounds are only poorly soluble in water and partly unstable in DMSO, the experiments were performed using ethanol as an additional solvent. A two-fold dilution method (CLSI, 2017[24]) was used resulting in an ethanol concentration ranging from 10% v/v to 0.08% v/v and compound concentrations between 0.5 mg mL^{-1} to 3.9 μg mL^{-1}. In order to test the influence of EtOH on the inhibition of bacterial growth, control experiments without the compound but with the respective EtOH concentrations were performed. Even though EtOH did display some inhibitory activity at the applied concentrations, the growth inhibition in the presence of some of the compounds was much higher compared to pure EtOH. Thus, these results can be seen as a first qualitative trend. For comparison, the graphics (Figures 6–8) show the untreated growth (in 8 different wells, black dashed line, squares) and the growth under the influence of the respective EtOH concentration (grey dashed line, circles). Strictly speaking, the x-axis scaling and labelling are not valid for these two graphs, as for the untreated growth the compound- and EtOH-concentration is 0 for all data points (black squares) and in the control experiment the EtOH concentration varies from 10% v/v to 0.08% v/v (grey circles). The triazoles tested in this work did not display any appreciable antibacterial activity against the Gram-negative bacterial strain *S. typhimurium*. Therefore, the results on the triazoles will not be discussed here any further. Under the condition of our testing, a similar behaviour was observed

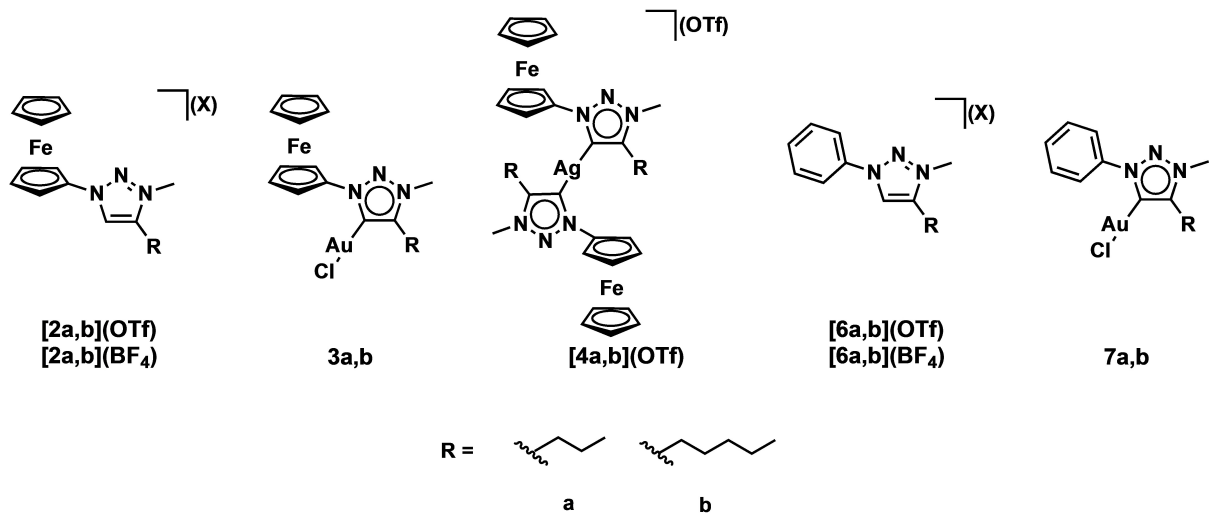

Figure 5. Selected compound library.

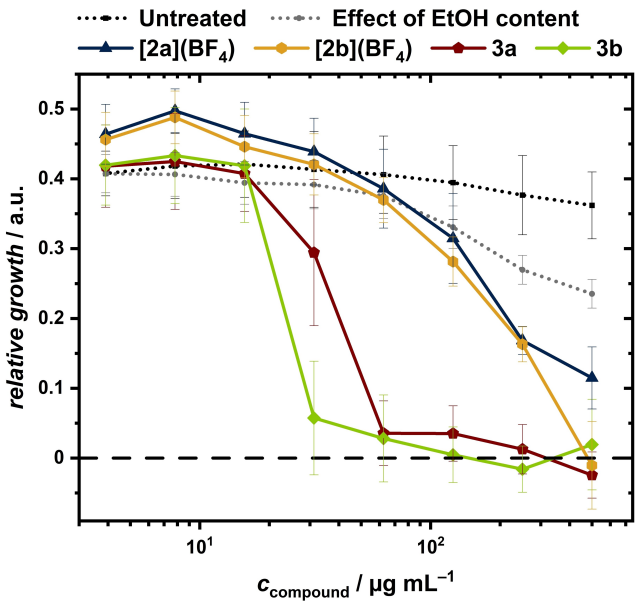

Figure 6. Effect of different compound concentrations of **[2a](BF$_4$)**, **[2b](BF$_4$)**, **3a** and **3b** on relative growth of *Salmonella typhimurium* after 20 h at 37 °C.

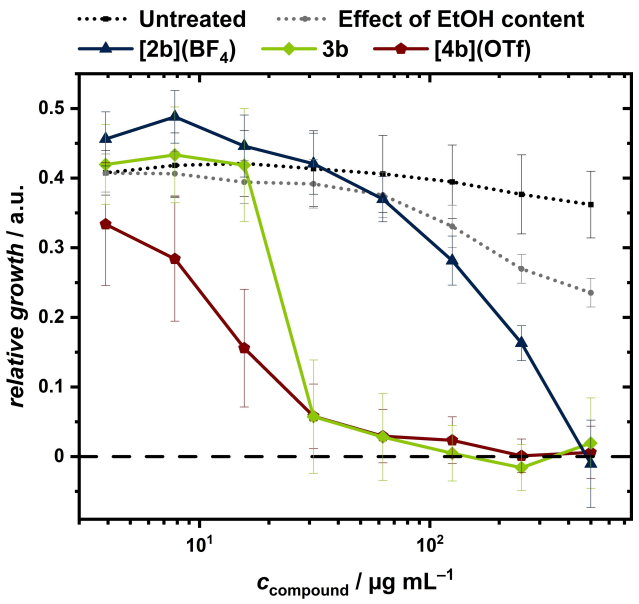

Figure 8. Effect of different compound concentrations of **[2b](BF$_4$)**, **3b** and **[4b](OTf)** on relative growth of *Salmonella typhimurium* after 20 h at 37 °C.

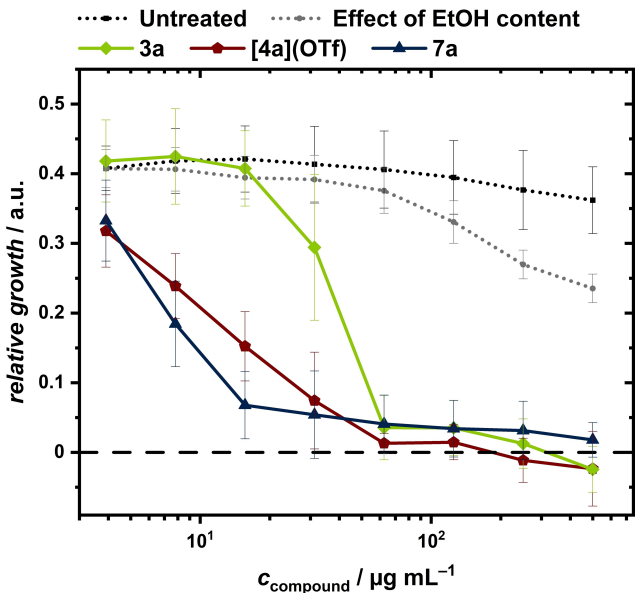

Figure 7. Effect of different compound concentrations of **3a**, **[4a](OTf)** and **7a** on relative growth of *Salmonella typhimurium* after 20 h at 37 °C.

for the triazolium salts affecting the bacterial growth only at high compound concentrations. No obvious trend concerning the counter ion or the aromatic substituent at N1 was observable (Table S11). However, a comparison of **[2a](BF$_4$)**, **[2b](BF$_4$)**, **3a** and **3b** (Figure 6) showed that the compounds containing the longer pentyl chain display (within their compound class) a slightly better activity compared to those containing the propyl chain.

When comparing the compounds **3a**, **[4a](OTf)** and **7a** it is seen that the compounds containing a phenyl substituent at the C4-position of the triazolylidene ring display better antibacterial activity compared to the compounds containing a ferrocenyl substituent (Figure 7). Contrary to the actual assumption, this indicates that the incorporation of the ferrocenyl group in this case negatively affects the antibacterial activity.

Finally, a comparison among the triazolium salt **[2b](BF$_4$)**, the gold(I) complex **3b** and the silver(I) complex **[4b](OTf)** demonstrates that the order of antibacterial activity for these compound classes is triazolium < Au(I) < Ag(I) (Figure 8). Even though for the compounds investigated here, the Ag(I) complex outperforms the Au(I) complex in terms of antibacterial activity, this does not seem to be a general trend, as an opposite trend has also been observed previously. These results thus clearly show the antibacterial activity of these compounds against the relatively resistant Gram-negative bacterial strain *S. typhimurium*, and also display the benefit of incorporating metals such as Ag(I) and Au(I) for improving antibacterial activity.

Finally, we were also interested in testing the antibacterial effect against the Gram-negative bacterial strain *E. coli*. In a preliminary study, qualitative data on bacterial growth under the influence of the compounds shown in Figure 5 were obtained by disc diffusion tests ($c = 1$ to 0.25 mg mL^{-1}). For comparison purposes, we also tested the effect of the established antibiotic kanamycin as well as of $AgNO_3$ under the same conditions. The EtOH concentration used did not contribute to the inhibition of growth of the *E. coli* strain. Similar to what has been observed for *S. typhimurium*, the triazolium salts did no inhibit the bacterial growth at the tested compound concentrations (Table S12). Only the silver(I) complexes **[4a, b](OTf)** and the gold(I) complexes **7a, b** showed a clear zone of inhibition. As for the growth of *S. typhimurium*, the

silver(I) complexes have the most potent effect on *E. coli* (Table S12). For the most promising candidates, namely **[4a, b](OTf)** and **7a**, antibacterial activity was further investigated by liquid microdilution testing. In this case, lower compound concentrations were chosen in order to avoid the impact of colour change on optical density measurements after incubation (please compare SI 6.1.1). As can be seen from Figure 9, the compounds inhibit bacterial growth only at a much higher concentration compared to both kanamycin and $AgNO_3$. Interestingly, the concentrations at which the tested compounds (particularly the metal complexes) display antibacterial activity against *S. typhimurium* is lower compared to the concentration at which the compounds affect the growth of *E. coli*. This result should also be valid despite the small growth-inhibiting effect of EtOH on the *Salmonella* strain.

Conclusion

In summary, we have presented here an investigation involving eight triazoles, seventeen triazolium salts, four gold(I)- and two silver(I) complexes. The synthesis and the thorough characterization of these compounds, including through single crystal X-ray diffraction studies have been presented. The ferrocenyl-containing compounds display a ferrocenyl-based oxidation step and an irreversible triazolium or triazolylidene based reduction step. The compounds were tested for their antibacterial activity against the Gram-negative bacterial strains *Salmonella typhimurium* and *Escherichia coli*. It was shown that especially the triazolylidene complexes display good antibacterial activity against the otherwise quite resistant *Salmonella* strain. The following trend with regard to the growth-inhibiting effect of the tested compounds was found: 1,2,3-triazole ≪ 1,2,3-triazolium salt < Au(I)-triazolylidene complexes < Ag(I)-triazolylidene complexes. To inhibit the growth of *Escherichia coli*, comparatively higher concentrations of the compounds studied here were required. Future work could involve the development of the triazolylidenes with functionalities such as –OH and –COOH as viable ligands for transition metals. Finding new synthetic strategies will be very important here, as these ligands will potentially increase the water solubility of the resulting metal complexes. Additionally, the resulting complexes can be important compounds for the studies of proton-coupled electron transfer (–OH/–COOH and ferrocenyl), with consequences for homogeneous catalysis. Further efforts will be necessary to improve the stability of such metal complexes, and to decipher the mode of action of their antibacterial activity. We have presented here a first qualitative study on the antibacterial activity of a set of 1,2,3-triazolium salts, and more important of the gold(I)- and silver(I)-MIC complexes.

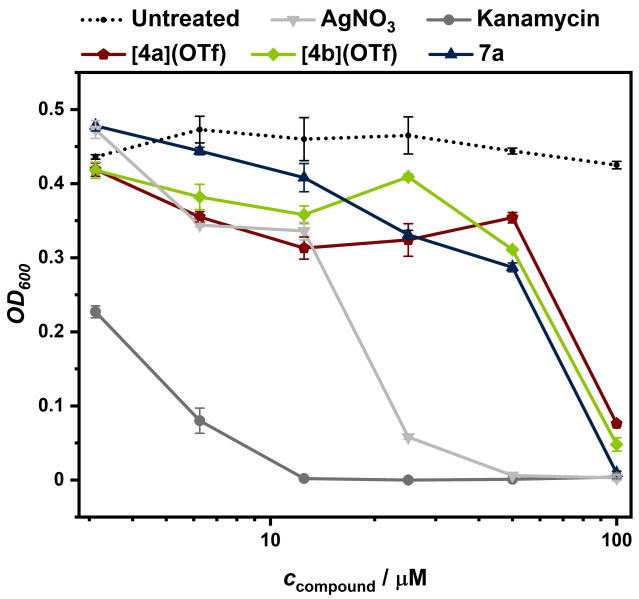

Figure 9. Optical Density (OD_{600}) as measure for bacterial growth of *E. coli* after 16 h at 37 °C and treatment with different compound concentrations of **[4a](OTf)**, **[4b](OTf)**, **7a**, **$AgNO_3$**, **Kanamycin** and without antibiotic (**untreated**).

Experimental Section

General Remarks and Instrumentation

All reactions, except CuAACs, were carried out using common Schlenk-line techniques under an inert atmosphere of nitrogen (Linde, HiQ Nitrogen 5.0, purity 99.999%). The solvents used for methylations and metal complex syntheses were available from a MBRAUN MB-SPS-800 solvent system. THF for cyclic voltammetry was dried and distilled from sodium/benzophenone under nitrogen. All absolute solvents were degassed by common techniques prior to use.

Commercially available chemicals were used as purchased. Bromoferrocene,[25] ferrocenyl azide,[26] phenyl azide,[27] AuCl(SMe_2)[28] and Ag_2O[29] were prepared as described previously in the literature.

Column chromatography was performed on Silica 60 M (0.04–0.063 mm).

Solvents were removed by rotary evaporation at 40 °C and appropriate pressure or under reduced pressure by exposing to vacuum (1×10^{-3} mbar).

^1H and $^{13}C\{^1H\}$ NMR spectra were recorded on Jeol ECS 400, Jeol ECZ 400, Jeol ECP 500, Bruker Avance 500, Jeol ECZ 600 or Bruker Avance 700 spectrometers at 20 °C. Chemical shifts are reported in parts per million (relative to the tetramethylsilane signal) with reference to the residual solvent peaks. The multiplicities and coupling constants are specified phenomenologically, i.e. according to the actual appearance of the signal and not according to the theoretically expected one. Multiplicities are reported as follows: singlet (s), doublet (d), triplet (t), quartet (q), quintet (p), sextet (sext) and multiplet (m). Connectivity was determined by ^1H, ^1H COSY, ^1H, ^{13}C HMBC and ^1H, ^{13}C HMQC experiments and in analogy to the literature.

Mass spectrometry was performed on an Agilent 6210 ESI-TOF.

X-ray data were collected on a Bruker D8 Venture diffractometer at 100(2) K using graphite monochromated Mo-K_α radiation (λ_α = 0.71073 Å). The strategy for the data collection was evaluated by using the APEX2[30] (**1c–d**, **[2b–d](OTf)**, **3a**, **[4a](OTf)**) or APEX3[31] (**[4b](OTf)**, **7a, b**) software. The data were collected by ω- and φ-

scan techniques and were scaled and reduced using Saint+[32] and SADABS[33] software. The structures were solved by intrinsic phasing methods using SHELXT-2014/4[34] (**1 c–d**, **[2 b–d](OTf)**, **3 a**), SHELXT-2014/5[34] (**[4 a](OTf)**), SHELXT-2017/1[34] (**[4 b](OTf)**, **7 a**) or Olex2[35] (**7 b**) and refined by full matrix least-squares using SHELXL-2014/7[36] (**1 c–d**, **[2 b–d](OTf)**, **3 a**, **[4 a](OTf)**), SHELXL-2017/1[36] (**[4 b](OTf)**, **7 a**) or SHELXL-2018/3[36] (**7 b**), refining on F^2. Non-hydrogen atoms were refined anisotropically. Molecular structures were visualized with the software Diamond.[37]

Cyclic voltammograms were recorded with a PAR VersaStat 4 potentiostat (Ametek) with a conventional three-electrode configuration consisting of a glassy carbon working electrode, a coiled platinum wire as counter electrode and a coiled silver wire as a pseudo reference electrode. All measurements were performed at room temperature with a scan rate of 100 mV/s. The experiments were carried out in absolute THF containing 0.1 M Bu_4NPF_6 (Fluka, $\geq$99.0 %, electrochemical grade) as the supporting electrolyte. Decamethylferrocene was added as internal reference. Potentials are reported against the ferrocene/ferrocenium couple.[38]

A detailed description of the synthesis and characterization of all the reported compounds can be found in the supporting information.

Deposition Numbers 1552960 (for **1 c**), 1552961 (for **1 e**), 1552965 (for **[2 c](OTf)**), 1552968 (for **[2 d](OTf)**), 1552974 (for **[2 b](OTf)**), 1552919 (for **[4 a](OTf)**), 2060754 (for **[4 b](OTf)**), 1552963 (for **3 a**), 2060755 (for **7 a**), and 2060756 (for **7 b**) contain the supplementary crystallographic data for this paper. These data are provided free of charge by the joint Cambridge Crystallographic Data Centre and Fachinformationszentrum Karlsruhe Access Structures service www.ccdc.cam.ac.uk/structures.

Acknowledgements

We would like to thank the Core Facility BioSupraMol, supported by the DFG, for assistance with NMR und ESI-MS measurements. Open access funding enabled and organized by Projekt DEAL.

Conflict of Interest

The authors declare no conflict of interest.

Keywords: Antibacterial agents · Carbene ligands · Ferrocenes · Silver · Triazoles

[1] a) R. Huisgen, R. Knorr, L. Möbius, G. Szeimies, *Chem. Ber.* **1965**, *98*, 4014–4021; b) R. Huisgen, G. Szeimies, L. Möbius, *Chem. Ber.* **1967**, *100*, 2494–2507; c) W. P. Fehlhammer, W. Beck, *Z. Anorg. Allg. Chem.* **2015**, *641*, 1599–1678; d) V. V. Rostovtsev, L. G. Green, V. V. Fokin, K. B. Sharpless, *Angew. Chem. Int. Ed.* **2002**, *41*, 2596–2599; *Angew. Chem.* **2002**, *114*, 2708–2711; e) L. Liang, D. Astruc, *Coord. Chem. Rev.* **2011**, *255*, 2933–2945; f) C. W. Tornoe, C. Christensen, M. Meldal, *J. Org. Chem.* **2002**, *67*, 3057–3064.

[2] H. C. Kolb, M. G. Finn, K. B. Sharpless, *Angew. Chem. Int. Ed.* **2001**, *40*, 2004–2021; *Angew. Chem.* **2001**, *113*, 2056–2075.

[3] a) G. Guisado-Barrios, M. Soleilhavoup, G. Bertrand, *Acc. Chem. Res.* **2018**, *51*, 3236–3244; b) S. Klenk, L. Suntrup, B. Sarkar, *Nachr. Chem.* **2018**, *66*, 717–721; c) D. Schweinfurth, L. Hettmanczyk, L. Suntrup, B. Sarkar, *Z. Anorg. Allg. Chem.* **2017**, *643*, 554–584; d) A. Vivancos, C. Segarra, M. Albrecht, *Chem. Rev.* **2018**, *118*, 9493–9586.

[4] a) A. Bolje, S. Hohloch, J. Kosmrlj, B. Sarkar, *Dalton Trans.* **2016**, *45*, 15983–15993; b) J. Bouffard, B. K. Keitz, R. Tonner, V. Lavallo, G. Guisado-Barrios, G. Frenking, R. H. Grubbs, G. Bertrand, *Organometallics* **2011**, *30*, 2617–2627; c) A. A. De la Fuente-Olvera, O. R. Suárez-Castillo, D. Mendoza-Espinosa, *Eur. J. Inorg. Chem.* **2019**, 4879–4886; d) S. N. R. Donthireddy, P. Mathoor Illam, A. Rit, *Inorg. Chem.* **2020**, *59*, 1835–1847; e) L. Hettmanczyk, L. Suntrup, S. Klenk, C. Hoyer, B. Sarkar, *Chem. Eur. J.* **2017**, *23*, 576–585; f) S. Hohloch, L. Suntrup, B. Sarkar, *Organometallics* **2013**, *32*, 7376–7385; g) M. Hollering, M. Albrecht, F. E. Kühn, *Organometallics* **2016**, *35*, 2980–2986; h) W. Huang, Y.-C. Zhang, R. Jin, B.-L. Chen, Z. Chen, *Organometallics* **2018**, *37*, 3196–3209; i) S. Klenk, S. Rupf, L. Suntrup, M. van der Meer, B. Sarkar, *Organometallics* **2017**, *36*, 2026–2035; j) K. O. Marichev, S. A. Patil, A. Bugarin, *Tetrahedron* **2018**, *74*, 2523–2546; k) D. Rendon-Nava, J. M. Vasquez-Perez, C. I. Sandoval-Chavez, A. Alvarez-Hernandez, D. Mendoza-Espinosa, *Organometallics* **2020**, *39*, 3961–3971; l) I. Strydom, G. Guisado-Barrios, I. Fernandez, D. C. Liles, E. Peris, D. I. Bezuidenhout, *Chem. Eur. J.* **2017**, *23*, 1393–1401; m) L. Suntrup, S. Hohloch, B. Sarkar, *Chem. Eur. J.* **2016**, *22*, 18009–18018; n) Á. Vivancos, M. Beller, M. Albrecht, *ACS Catal.* **2017**, *8*, 17–21; o) S. Hohloch, D. Scheiffele, B. Sarkar, *Eur. J. Inorg. Chem.* **2013**, 3956–3965; p) S. Hohloch, C.-Y. Su, B. Sarkar, *Eur. J. Inorg. Chem.* **2011**, 3067–3075; q) L. Suntrup, J. Beerhues, O. Etzold, B. Sarkar, *Dalton Trans.* **2020**, *49*, 15504–15510; r) J. Beerhues, K. Fauche, F. Cisnetti, B. Sarkar, A. Gautier, *Dalton Trans.* **2019**, *48*, 8931–8936; s) S. Vanicek, J. Beerhues, T. Bens, V. Levchenko, K. Wurst, B. Bildstein, M. Tilset, B. Sarkar, *Organometallics* **2019**, *38*, 4383–4386.

[5] a) V. Leigh, W. Ghattas, R. Lalrempuia, H. Muller-Bunz, M. T. Pryce, M. Albrecht, *Inorg. Chem.* **2013**, *52*, 5395–5402; b) M. van der Meer, E. Glais, I. Siewert, B. Sarkar, *Angew. Chem. Int. Ed.* **2015**, *54*, 13792–13795; *Angew. Chem.* **2015**, *127*, 13997–14000; c) R. Maity, M. van der Meer, B. Sarkar, *Dalton Trans.* **2015**, *44*, 46–49.

[6] a) S. Sinn, B. Schulze, C. Friebe, D. G. Brown, M. Jager, E. Altuntas, J. Kubel, O. Guntner, C. P. Berlinguette, B. Dietzek, U. S. Schubert, *Inorg. Chem.* **2014**, *53*, 2083–2095; b) L. Suntrup, F. Stein, J. Klein, A. Wilting, F. G. L. Parlane, C. M. Brown, J. Fiedler, C. P. Berlinguette, I. Siewert, B. Sarkar, *Inorg. Chem.* **2020**, *59*, 4215–4227; c) L. Suntrup, F. Stein, G. Hermann, M. Kleoff, M. Kuss-Petermann, J. Klein, O. S. Wenger, J. C. Tremblay, B. Sarkar, *Inorg. Chem.* **2018**, *57*, 13973–13984; d) S. Sinn, B. Schulze, C. Friebe, D. G. Brown, M. Jager, J. Kubel, B. Dietzek, C. P. Berlinguette, U. S. Schubert, *Inorg. Chem.* **2014**, *53*, 1637–1745; e) A. R. Naziruddin, C. S. Lee, W. J. Lin, B. J. Sun, K. H. Chao, A. H. Chang, W. S. Hwang, *Dalton Trans.* **2016**, *45*, 5848–5859; f) J. Soellner, M. Tenne, G. Wagenblast, T. Strassner, *Chem. Eur. J.* **2016**, *22*, 9914–9918; g) L. Hettmanczyk, S. J. P. Spall, S. Klenk, M. van der Meer, S. Hohloch, J. A. Weinstein, B. Sarkar, *Eur. J. Inorg. Chem.* **2017**, 2112–2121; h) P. Chabera, Y. Liu, O. Prakash, E. Thyrhaug, A. E. Nahhas, A. Honarfar, S. Essen, L. A. Fredin, T. C. Harlang, K. S. Kjaer, K. Handrup, F. Ericson, H. Tatsuno, K. Morgan, J. Schnadt, L. Haggstrom, T. Ericsson, A. Sobkowiak, S. Lidin, P. Huang, S. Styring, J. Uhlig, J. Bendix, R. Lomoth, V. Sundstrom, P. Persson, K. Warnmark, *Nature* **2017**, *543*, 695–699; i) B. Sarkar, L. Suntrup, *Angew. Chem. Int. Ed.* **2017**, *56*, 8938–8940; *Angew. Chem.* **2017**, *129*, 9064–9066; j) E. Matteucci, F. Monti, R. Mazzoni, A. Baschieri, C. Bizzarri, L. Sambri, *Inorg. Chem.* **2018**, *57*, 11673–11686.

[7] a) L. Hettmanczyk, S. Manck, C. Hoyer, S. Hohloch, B. Sarkar, *Chem. Commun.* **2015**, *51*, 10949–10952; b) S. Vanicek, M. Podewitz, J. Stubbe, D. Schulze, H. Kopacka, K. Wurst, T. Muller, P. Lippmann, S. Haslinger, H. Schottenberger, K. R. Liedl, I. Ott, B. Sarkar, B. Bildstein, *Chem. Eur. J.* **2018**, *24*, 3742–3753.

[8] a) M. Flores-Jarillo, D. Mendoza-Espinosa, V. Salazar-Pereda, S. González-Montiel, *Organometallics* **2017**, *36*, 4305–4312; b) M. Frutos, M. G. Avello, A. Viso, R. Fernandez de la Pradilla, M. C. de la Torre, M. A. Sierra, H. Gornitzka, C. Hemmert, *Org. Lett.* **2016**, *18*, 3570–3573; c) L. Hettmanczyk, D. Schulze, L. Suntrup, B. Sarkar, *Organometallics* **2016**, *35*, 3828–3836; d) K. J. Kilpin, U. S. Paul, A. L. Lee, J. D. Crowley, *Chem. Commun.* **2011**, *47*, 328–330; e) D. Mendoza-Espinosa, R. González-Olvera, G. E. Negrón-Silva, D. Angeles-Beltrán, O. R. Suárez-Castillo, A. Álvarez-Hernández, R. Santillan, *Organometallics* **2015**, *34*, 4529–4542; f) D. Mendoza-Espinosa, D. Rendon-Nava, A. Alvarez-Hernandez, D. Angeles-Beltran, G. E. Negron-Silva, O. R. Suarez-Castillo, *Chem. Asian J.* **2017**, *12*, 203–207; g) A. Priante-Flores, V. Salazar-Pereda, A. L. Rheingold, D. Mendoza-Espinosa, *New J. Chem.* **2018**, *42*, 15533–15537.

[9] K. F. Donnelly, A. Petronilho, M. Albrecht, *Chem. Commun.* **2013**, *49*, 1145–1159.

[10] R. Heath, H. Muller-Bunz, M. Albrecht, *Chem. Commun.* **2015**, *51*, 8699–8701.

[11] a) K. Bozorov, J. Zhao, H. A. Aisa, *Bioorg. Med. Chem.* **2019**, *27*, 3511–3531; b) X. M. Chu, C. Wang, W. L. Wang, L. L. Liang, W. Liu, K. K. Gong, K. L. Sun, *Eur. J. Med. Chem.* **2019**, *166*, 206–223; c) F. de Carvalho da Silva, M. F. C. Cardoso, P. G. Ferreira, V. F. Ferreira, in *Chemistry of 1,2,3-triazoles*. Topics in Heterocyclic Chemistry, Vol. 40 (Eds.: W. Dehaen, V. Bakulev), Springer, **2014**, 117–165; d) A. Rani, G. Singh, A. Singh, U. Maqbool, G. Kaur, J. Singh, *RSC Adv.* **2020**, *10*, 5610–5635; e) S. H. Sumrra, U. Habiba, W. Zafar, M. Imran, Z. H. Chohan, *J. Coord. Chem.* **2020**, *73*, 2838–2877; f) M. Xu, Y. Peng, L. Zhu, S. Wang, J. Ji, K. P. Rakesh, *Eur. J. Med. Chem.* **2019**, *180*, 656–672; g) B. Zhang, *Eur. J. Med. Chem.* **2019**, *168*, 357–372.

[12] a) B. Dominelli, J. D. G. Correia, F. E. Kühn, *J. Organomet. Chem.* **2018**, *866*, 153–164; b) J. C. Garrison, W. J. Youngs, *Chem. Rev.* **2005**, *105*, 3978–4008; c) K. M. Hindi, M. J. Panzner, C. A. Tessier, C. L. Cannon, W. J. Youngs, *Chem. Rev.* **2009**, *109*, 3859–3884; d) M. G. Karaaslan, A. Aktas, C. Gurses, Y. Gok, B. Ates, *Bioorg. Chem.* **2020**, *95*, 103552; e) O. Karaca, S. M. Meier-Menches, A. Casini, F. E. Kuhn, *Chem. Commun.* **2017**, *53*, 8249–8260; f) A. Kascatan-Nebioglu, M. J. Panzner, C. A. Tessier, C. L. Cannon, W. J. Youngs, *Coord. Chem. Rev.* **2007**, *251*, 884–895; g) W. Liu, R. Gust, *Coord. Chem. Rev.* **2016**, *329*, 191–213; h) I. Ott, in *Inorganic and Organometallic Transition Metal Complexes with Biological Molecules and Living Cells*, Ed. K. K.-W. Lo, Academic Press, **2017**, 147–179; i) M. Porchia, M. Pellei, M. Marinelli, F. Tisato, F. Del Bello, C. Santini, *Eur. J. Med. Chem.* **2018**, *146*, 709–746; j) N. Touj, I. S. A. Nasr, W. S. Koko, T. A. Khan, I. Özdemir, S. Yasar, L. Mansour, F. Alresheedi, N. Hamdi, *J. Coord. Chem.* **2020**, *73*, 2889–2905; k) S. A. Patil, S. A. Patil, R. Patil, R. S. Keri, S. Budagumpi, G. R. Balakrishna, M. Tacke, *Future Med. Chem.* **2015**, *7*, 1305–1333; l) S. A. Patil, A. P. Hoagland, S. A. Patil, A. Bugarin, *Future Med. Chem.* **2020**, *12*, 2239–2275.

[13] a) J. T. Fletcher, J. M. Sobczyk, S. C. Gwazdacz, A. J. Blanck, *Bioorg. Med. Chem. Lett.* **2018**, *28*, 3320–3323; b) R. S. Meinel, A. D. C. Almeida, P. H. F. Stroppa, N. Glanzmann, E. S. Coimbra, A. D. da Silva, *Chem.-Biol. Interact.* **2020**, *315*, 108850; c) J. P. Shrestha, C. W. Chang, *Bioorg. Med. Chem. Lett.* **2013**, *23*, 5909–5911; d) R. Shyam, N. Charbonnel, A. Job, C. Blavignac, C. Forestier, C. Taillefumier, S. Faure, *ChemMedChem* **2018**, *13*, 1513–1516; e) I. Steiner, N. Stojanovic, A. Bolje, A. Brozovic, D. Polancec, A. Ambriovic-Ristov, M. R. Stojkovic, I. Piantanida, D. Eljuga, J. Kosmrlj, M. Osmak, *Radiol. Oncol.* **2016**, *50*, 280–288; f) P. H. F. Stroppa, L. M. R. Antinarelli, A. M. L. Carmo, J. Gameiro, E. S. Coimbra, A. D. da Silva, *Bioorg. Med. Chem.* **2017**, *25*, 3034–3045; g) W. Tan, Q. Li, F. Dong, J. Zhang, F. Luan, L. Wei, Y. Chen, Z. Guo, *Carbohydr. Polym.* **2018**, *182*, 180–187; h) W. Tan, J. Zhang, F. Luan, L. Wei, Q. Li, F. Dong, Z. Guo, *Int. J. Biol. Macromol.* **2017**, *101*, 845–851; i) R. Wang, Y. Li, W. Dehaen, *Eur. J. Med. Chem.* **2020**, *207*, 112737.

[14] a) D. Aucamp, S. V. Kumar, D. C. Liles, M. A. Fernandes, L. Harmse, D. I. Bezuidenhout, *Dalton Trans.* **2018**, *47*, 16072–16081; b) K. J. Kilpin, S. Crot, T. Riedel, J. A. Kitchen, P. J. Dyson, *Dalton Trans.* **2014**, *43*, 1443–1448; c) J. Kralj, A. Bolje, D. S. Polančec, I. Steiner, T. Gržan, A. Tupek, N. Stojanović, S. Hohloch, D. Urankar, M. Osmak, B. Sarkar, A. Brozovic, J. Košmrlj, *Organometallics* **2019**, *38*, 4082–4092.

[15] S. D. Koester, J. Dittrich, G. Gasser, N. Huesken, I. C. Henao Castaneda, J. L. Jios, C. O. Della Vedova, N. Metzler-Nolte, *Organometallics* **2008**, *27*, 6326–6332.

[16] a) A. Kolarovic, M. Schnurch, M. D. Mihovilovic, *J. Org. Chem.* **2011**, *76*, 2613–2618; b) H. A. Stefani, H. A. Canduzini, F. Manarin, *Tetrahedron Lett.* **2011**, *52*, 6086–6090.

[17] a) G. Gasser, N. Metzler-Nolte, *Curr. Opin. Chem. Biol.* **2012**, *16*, 84–91; b) C. G. Hartinger, P. J. Dyson, *Chem. Soc. Rev.* **2009**, *38*, 391–401; c) M. Patra, G. Gasser, *Nat. Chem. Rev.* **2017**, *1*, 1–12; d) S. Sansook, S. Hassell-Hart, C. Ocasio, J. Spencer, *J. Organomet. Chem.* **2020**, *905*; e) A. Singh, I. Lumb, V. Mehra, V. Kumar, *Dalton Trans.* **2019**, *48*, 2840–2860.

[18] A. Bolje, D. Urankar, J. Košmrlj, *Eur. J. Org. Chem.* **2014**, 8167–8181.

[19] A. Bolje, S. Hohloch, D. Urankar, A. Pevec, M. Gazvoda, B. Sarkar, J. Košmrlj, *Organometallics* **2014**, *33*, 2588–2598.

[20] D. Schweinfurth, R. Pattacini, S. Strobel, B. Sarkar, *Dalton Trans.* **2009**, 9291–9297.

[21] J. R. Wright, P. C. Young, N. T. Lucas, A. L. Lee, J. D. Crowley, *Organometallics* **2013**, *32*, 7065–7076.

[22] a) J. C. Y. Lin, R. T. W. Huang, C. S. Lee, A. Bhattacharyya, W. S. Hwang, I. J. B. Lin, *Chem. Rev.* **2009**, *109*, 3561–3598; b) T. V. Serebryanskaya, A. A. Zolotarev, I. Ott, *Med. Chem. Commun.* **2015**, *6*, 1186–1189; c) J. Turek, I. Panov, P. Svec, Z. Ruzickova, A. Ruzicka, *Dalton Trans.* **2014**, *43*, 15465–15474; d) J. Turek, Z. Růžičková, A. Růžička, *Inorg. Chem. Commun.* **2014**, *48*, 103–106.

[23] a) J. Cai, X. Yang, K. Arumugam, C. W. Bielawski, J. L. Sessler, *Organometallics* **2011**, *30*, 5033–5037; b) E. C. Keske, O. V. Zenkina, R. Wang, C. M. Crudden, *Organometallics* **2012**, *31*, 456–461.

[24] Clinical and Laboratory Standards Institute, **2017**. Performance Standards for Antimicrobial Susceptibility Testing: Twenty-seventh Informational Supplement M100-S27. CLSI, Wayne PA, USA.

[25] D. A. Khobragade, S. G. Mahamulkar, L. Pospisil, I. Cisarova, L. Rulisek, U. Jahn, *Chem. Eur. J.* **2012**, *18*, 12267–12277.

[26] A. Shafir, M. P. Power, G. D. Whitener, J. Arnold, *Organometallics* **2000**, *19*, 3978–3982.

[27] S. W. Kwok, J. R. Fotsing, R. J. Fraser, V. O. Rodionov, V. V. Fokin, *Org. Lett.* **2010**, *12*, 4217–4219.

[28] T. N. Hooper, C. P. Butts, M. Green, M. F. Haddow, J. E. McGrady, C. A. Russell, *Chem. Eur. J.* **2009**, *15*, 12196–12200.

[29] W. Huang, R. Zhang, G. Zou, J. Tang, J. Sun, *J. Organomet. Chem.* **2007**, *692*, 3804–3809.

[30] Bruker, *APEX2*. Bruker AXS Inc., Madison, Wisconsin, USA, **2012**.

[31] Bruker, *APEX3*. Bruker AXS Inc., Madison, Wisconsin, USA, **2015**.

[32] Bruker, *SAINT+*. Bruker AXS Inc., Madison, Wisconsin, USA, **2009**.

[33] Bruker, *SADABS*. Bruker AXS Inc., Madison, Wisconsin, USA, **2008**.

[34] G. M. Sheldrick, *Acta Crystallogr. Sect. A* **2015**, *71*, 3–8.

[35] O. V. Dolomanov, L. J. Bourhis, R. J. Gildea, J. A. K. Howard, H. Puschmann, *J. Appl. Crystallogr.* **2009**, *42*, 339–341.

[36] G. M. Sheldrick, *Acta Crystallogr. Sect. C* **2015**, *71*, 3–8.

[37] K. Brandenburg, H. Putz, *DIAMOND*, Crystal and Molecular Structure Visualization; Crystal Impact GbR, Bonn, Germany, **2014**.

[38] J. A. Aranzaes, M.-C. Daniel, D. Astruc, *Can. J. Chem.* **2006**, *84*, 288–299.

Manuscript received: January 12, 2021
Revised manuscript received: February 10, 2021
Accepted manuscript online: February 17, 2021